HHS Public Access

Author manuscript

Nucl Med Biol. Author manuscript; available in PMC 2015 August 06.

Published in final edited form as:

Nucl Med Biol. 2011 July ; 38(5): 675–681. doi:10.1016/j.nucmedbio.2010.12.011.

IN VIVO BIODISTRIBUTION AND ACCUMULATION OF ^{89}Zr IN MICE

D.S. Abou[1], **T. Ku**[1], and **P.M. Smith-Jones**[1,2]

[1]Department of Radiology, Radiochemistry Service, Memorial Sloan Kettering Cancer Center, 1275 York Avenue, Box 16, New York, NY 10065

[2]University of Colorado Denver, Leprino Building, Department of Radiology, L954, 12401 E. 17th Ave, Aurora, CO 80045

Abstract

Introduction—The present investigation focuses on the chemical and biological fate of ^{89}Zr in mice. Electrophoreses of ^{89}Zr solvated or chelated in different conditions are here presented. The biological fate of mice injected with [^{89}Zr]Zr-oxalate, [^{89}Zr]Zr-chloride, [^{89}Zr]Zr-phosphate, [^{89}Zr]Zr-desferrioxamine and [^{89}Zr]Zr-citrate is studied with the biodistribution, the clearances and PET images. A special focus is also given regarding the quality of ^{89}Zr bone accumulation.

Methods—Electrophoreses were carried out on chromatography paper and read by gamma counting. Then, the solutions were intravenously injected in mice, imaged at different time points and sacrificed. The bones, the epiphysis and the marrow substance were separated and evaluated with gamma counts.

Results—The clearances of [^{89}Zr]Zr-chloride and [^{89}Zr]Zr-oxalate reached 20% of ID after 6 days whereas [^{89}Zr]Zr-phosphate was only 5% of ID. [^{89}Zr]Zr-citrate and [^{89}Zr]Zr-DFO were noticeably excreted after the first day p.i.. [^{89}Zr]Zr-chloride and [^{89}Zr]Zr-oxalate resulted in a respective bone uptake of ~15% ID/g and~20% ID/g at 8 h p.i. with minor losses after 6 days. [^{89}Zr]Zr-citrate bone uptake was also observed, but [^{89}Zr]Zr-phosphate was absorbed in high amounts in the liver and the spleen. The marrow cells were insignificantly radioactive in comparison to the calcified tissues.

Conclusion—Despite the complexity of Zr coordination, the electrophoretic analyses provided detailed evidences of Zr charges either as salts or as complexes. This study also shows that weakly chelated, ^{89}Zr is a bone seeker and has a strong affinity for phosphate.

Keywords

PET; ^{89}Zr; chloride; oxalate; phosphate; bone seeker

Corresponding Author: Diane ABOU, Aboud@mskcc.org, Tel: 01-646-888-3081.

INTRODUCTION

Zirconium (Zr) was discovered by Klaproth in 1789 as zircon in the form of orthosilicate. It was first isolated as a metal by Berzelius in 1824. For a long time Zr was used in an impure form, that of zircon, with industrial applications that included fabrication of fake diamonds; but at that time, Zr was of very little attention in the medical field [1].

During the atomic testing period of the 1950's and 1960's, ^{93}Zr and ^{95}Zr emerged as important fission products. Much of the early studies of the radiochemistry of zirconium were published in the 1960 NAS report [2]. One major point in the publication was that $ZrO(PO_4)_2$ had a solubility product of 2.28×10^{-18} and that it could be precipitated in this form from 20% sulfuric acid. Zr has a common oxidation state of +4 and the hexaaqua ion $Zr(H_20)_6^{+4}$ only exists in very low Zr concentrations and in highly acidic aqueous solutions. In neutral solutions, in the absence of any complexing agents, Zr is mostly found as a polynuclear and polymeric form [3, 4].

The early interests in fission / fallout lead to animal studies to investigate the biological distribution of ^{93}Zr and ^{95}Zr in the 1950's and 1960's. These included the toxicity [5] and the biodistribution of ^{95}Zr in rats or in mice [6, 7]. These works showed the high affinity of Zr to the bones by autoradiography and its low toxicity in rats.

The last decade has seen a rising interest for the use of ^{89}Zr as a potential PET (Positron Emission Tomography) isotope for the labeling of monoclonal antibody for *in vivo* cancer imaging [8–11]. The long half-life of ^{89}Zr ($t_{1/2}$ = 78.41 hours) is compatible with the relatively slow blood clearance of most IgGs used in radioimmunodiagnosis ($t_{1/2}$ = 1–2 days). The slow blood clearance often means that the maximum tumor accumulation of an IgG at the tumor is around 3–5 days. The ^{89}Zr tracer is commonly attached via a desferrioxamine (DFO) moiety conjugated to the antibody. Two main conjugation methods are in use. One deals with a succinic acid linker between the amine of the DFO and an amine of the antibody [8] and the other involves a p-Isothiocyanatobenzyl-desferrioxamine derivative [12]. The latter method has the advantage of vastly simplifying the conjugation procedure using commercially available *p*-Isothiocyanatobenzyl-desferrioxamine and a one-step method.

This advantageous half-life and conjugation strategy has led to the development and the coming clinical trials of ^{89}Zr-DFO-J591 and ^{89}Zr-DFO-trasuzumab at MSKCC [9]. Despite the interest, a number of questions have arisen regarding the stability of the Zr-DFO complex in a long term study in physiological conditions (on the order of days). An increasing contrast of the bones was observed in mice three days following the ^{89}Zr-DFO-J591 injection (~9% ID/g) [9], which was not detected at such extended time points with labeled ^{111}In-DOTA-J591 or ^{177}Lu-DOTA-J591 [13, 14]. Therefore, the postulated high stability of Zr-DFO chelate conjugated to the antibody does not match with the observed non specific uptake of ^{89}Zr by the bones. It can be hypothesized that either the attachment of Zr-DFO to the antibody is not resistant enough after immuno-recognition or that the Zr is transmetallated.

The present study attempts to address these questions using electrophoresis characterization of ^{89}Zr solvated in different ionic conditions (in saline and in phosphate buffer saline) or ^{89}Zr chelated by different biologically relevant species such as oxalate, citrate or DFO and looking at the biological fate of these species. The biodistribution, clearances and imaging of each injection species are presented here and discussed. A special focus is also given regarding the bone accumulation of ^{89}Zr.

MATERIAL and METHODS

All chemicals were purchased at Sigma-Aldrich (St Louis, Mo, USA)

Preparation of [^{89}Zr]Zr-oxalate in (1M) oxalic acid

The purification and the isolation of ^{89}Zr was performed as described earlier [15]. The supplied [^{89}Zr]Zr-oxalate was neutralized with $NaCO_3$ [1M] and diluted with saline (0.9 % NaCl) to give a final oxalate concentration of 10 mM.

Preparation of [^{89}Zr]Zr-chloride

[^{89}Zr]Zr-oxalate (containing 10 μL of 1M oxalic acid) was evaporated to dryness 100–110°C under a stream of nitrogen and then digested with 20 μL of hydrochloric acid (37%) and 20 μL nitric acid (70%) (ratio 1:1). The mixture was then dried again at 100–110°C. This procedure was repeated several times. The residue was diluted in glacial acetic acid and heated until complete dryness. The resulting preparation was dissolved in saline. The final pH was 5.

Preparation of [^{89}Zr]Zr-phosphate

The same protocol as detailed above was followed for the preparation of [^{89}Zr]Zr-phosphate. A modification of the final step saw the addition of PBS (Phosphate Buffer Saline) in the place of saline. The pH of that preparation reached 6.

Preparation of [^{89}Zr]Zr-desferrioxamine (DFO) and [^{89}Zr]Zr-citrate

The [^{89}Zr]Zr chloride solution was mixed with an aqueous solution of 50 mM DFO or 50 mM of sodium citrate and the metal complex allowed to form at ambient temperature.

Characterization of the chemicals

Each preparation of the radionuclide was characterized using electrophoresis. The solutions were migrated on chromatography paper (Whatman paper 3MM CHR; Whatman Int. Ltd., Maidstone, EN). The strips were sized 203 mm length and 20 mm width, and the solutions spotted at the center of the strip (101.5 mm from its edge). The strips were bathed in acetate buffer (50 mM, pH=6.5) in a horizontal electrophoresis chamber submitted to a 220V and 10mA electric current delivered by a Hoefer Scientific instrument (Holliston, MA, USA) power supply. The electrophoresed strips were run for 3h, and were read using a Bioscan System 200 Imaging scanner (Washington, DC, USA). All these chromatograms were run twice and are displayed in Fig. 1 with the cathode standing on the left side and the anode on the right side of the strip.

In vivo experiments and PET Imaging

All animal experiments were performed following the rules and guidelines of the National Institute of Health (NIH) and the Institutional Animal Care and Use Committee [16]. Each trial was performed triplicate. Groups of female NIHS, were intravenously injected in the tail with [^{89}Zr]Zr chloride, [^{89}Zr]Zr-oxalate, [^{89}Zr]Zr-phosphate, [^{89}Zr]Zr-citrate and [^{89}Zr]Zr-DFO (740 KBq in 200μL). The mice were imaged (1, 3, 8, 24 hours and 6 days post injection (p.i) with 10 min scan length) under anesthesia by inhalation of 1% isoflurane (Baxter Healthcare, Deerfield, IL, USA) / oxygen gas mixture (flow rate: 2 L.min^{-1}) using micro-PET Focus® 120 scanner. PET scans were reconstructed with Concorde Microsystems software. Groups of animals, injected with [^{89}Zr]Zr-chloride, [^{89}Zr]Zr-oxalate and [^{89}Zr]Zr-phosphate were sacrificed and biodistribution studies were performed at 4 h, 8 h and 6 days p.i.. Those injected with [^{89}Zr]Zr-citrate and DFO were sacrificed and dissected at 6 days p.i.. The collected organs were weighed and measured, with ^{89}Zr standards, using a gamma counter (Wizard 1480, Perkin Elmer, Waltham, MA, USA) and the %ID/g of ^{89}Zr in each organ calculated. The whole body clearance of activity was also determined by repeatedly measuring each mouse in a dose calibrator (CRC127R, Capintec Inc., NJ, USA) over the course of the study.

Separation and activity distribution of the marrow cells and the bones

A representative group of mice with high bone uptake of ^{89}Zr were studied in more detail. The tibia and the femur of the mice were harvested. The epiphysis of both the femur and the tibia were first removed, then, the shafts of the femur and the tibia were flushed with a known volume and weight of saline in order to remove the marrow cells. The resulting solution was weighted and the extracted marrow was quantified by subtracting the original weight of saline. The bones, the epiphysis and the collected marrow substance were analyzed with a gamma count.

RESULTS

Electrophoresis of the chemical solutions

Fig. 1 displays the results of electrophoresis. It can be seen that [^{89}Zr]Zr-chloride (A) and [^{89}Zr]Zr-phosphate (C) have hardly migrated from their initial point, showing a thin sharp peak nearby the origin. This is indicative of non-charged species. [^{89}Zr]Zr-oxalate (B) showed a broader peak than [^{89}Zr]Zr-chloride. The peak stretches towards the anode due to being a positively charged species. A slight migration of the activity is also apparent, towards the cathode. As expected, [^{89}Zr]Zr-DFO electrophoresis (D) shows a peak of activity tending to the anode side, well-distinguished from the starting point and matching with the known charge of +2 for (Zr-DFO-Ms)$^{+2}$ [15]. Finally, [^{89}Zr]Zr-citrate displays signs of radioactivity indicative of both neutral and negatively charged species.

In vivo experiments: clearance and biodistribution

Fig. 2 displays the results of the activity retained in the body up to 6 days p.i. For all the of the chemical species, the profile of clearance appears as a relative flat line after the first day of injection, indicating a body activity constant up to 6 days. The clearances of [^{89}Zr]Zr-

chloride and [^{89}Zr]Zr-oxalate reached 20% of the ID after 6 days while [^{89}Zr]Zr-phosphate was hardly cleared following 6 days, with only 5% of activity loss. The mice injected with [^{89}Zr]Zr-citrate cleared about 30% of the ID the first day and 35% after 6 days. Finally, [^{89}Zr]Zr-DFO was completely excreted after the first day of injection.

The biodistribution results are presented Fig. 3 and 4. [^{89}Zr]Zr-chloride (A) and [^{89}Zr]Zr-oxalate (B) have similar profiles with an important activity uptake in the bones: ~20% ID/g for [^{89}Zr]Zr-oxalate and ~15% ID/g for [^{89}Zr]Zr-chloride over 8 h p.i. with a minor loss of bone activity of 2 to 3% after 6 days. A small difference is noted regarding the blood activity at 4 and 8 h p.i. with a higher amount for [^{89}Zr]Zr-oxalate (~8%ID/g) compare to [^{89}Zr]Zr-chloride (~4%ID/g). In both cases, the blood activity decreases dramatically after 6 days. Up to three hour p.i., the heart and the lungs also accumulated some activity (see the PET image, Fig. 5) disappearing after 6 days. [^{89}Zr]Zr-phosphate (C) was very quickly absorbed in high amounts in the liver and the spleen, likely due to a precipitate form of this compound. [^{89}Zr]Zr-phosphates bone activity was much weaker than that of [^{89}Zr]Zr-chloride and [^{89}Zr]Zr-oxalate.

A summary of the biodistribution results, for all of the species 6 days p.i. is found in Fig. 4. [^{89}Zr]Zr-chloride and [^{89}Zr]Zr-oxalate have bone uptake as the most significant constituents of accumulation with a very little activity lost post 6 days. The bone uptake of [^{89}Zr]Zr-citrate is also noticeable whereas the bone uptake of [^{89}Zr]Zr-phosphate is negligible. The high activity in the spleen and the liver for [^{89}Zr]Zr-phosphate indicates that this species has not been excreted, as correlated with the clearance (Fig. 2). The distribution of [^{89}Zr]Zr-DFO is barely detectable at this final time point in comparison to the other groups. Further, only the kidneys were slightly radioactive 6 days following the injection.

Focus on bones and bone marrows

More than 99 % of the whole sample activity was located in the bones and the epiphyses respectively 33% (0.96 % ID/g) and 66% of the whole bone activity (1.92 % ID/g). The extracted marrow cells were insignificantly radioactive in comparison to the calcified tissues (0.1% of the total activity of the bones).

DISCUSSION

The electrophoresis of [^{89}Zr]Zr-chloride is in accordance with reported studies describing the polynuclear and polymeric forms of Zr, when hydrolyzed in the near neutral pH region [3, 4]. When solvated in acetate buffer at pH=6.5, Zr may be octachelated likely by hydroxides, water molecules and chlorides resulting in a colloidal form. By the effect of mass of the polymeric structure, the Zr species stagnate at the origin as if the overall charge was neutral, probably due to a low charge / mass ratio (Fig. 1.A). However, investigations of the biodistribution results indicate very little activity accumulated in the liver and the spleen. This suggests that as soon as Zr is injected it is likely dissolved in the blood and loses its colloidal form. The blood activity measured after the first 8 h p.i. confirms this observation and matches previous data reporting that free zirconium binds plasma proteins [17]. The heart and the lungs, highly vascularized organs, also show a high activity with [^{89}Zr]Zr-chloride and [^{89}Zr]Zr-oxalate up to 8 h p.i. (Fig. 5). This activity was then rapidly cleared in

favor of an enhancement of the bone uptake. Indeed, Zr shows a high affinity for the bones as displayed in the PET images (Fig. 5), for example, the whole mouse backbone is clearly visible. The separation of the marrow cellular compartment from the bone also demonstrates the strong affinity of Zr for the bones and joints.

In the neutralized [^{89}Zr]Zr-oxalate preparation, Zr^{4+} is probably octachelated by four oxalates, resulting in an overall charge of −4 [18]. This hypothesis matches the anion displayed on electrophoresis results (Fig. 1-B). Alternatively, the positively charged species could be attributed to different forms of cationic Zr simultaneously chelated by a combination of hydroxides, water molecules and oxalates. Regarding Zr-oxalate clearance, only 20% is cleared after 6 days p.i. versus 35% for [^{89}Zr]Zr-citrate or 100% for [^{89}Zr]Zr-DFO. In the present case, when Zr is chelated, the radioactivity is significantly cleared from the mice body. The clearance of [^{89}Zr]Zr-oxalate (bidentate chelator [18]) is relevant as it resembles an unstable complex at physiological pH, in comparison to [^{89}Zr]Zr-citrate (tridentate chelator, moderately stable [19]) or [^{89}Zr]Zr-DFO (hexadentate chelator, stable complexes [20]). In addition, the biodistribution of [^{89}Zr]Zr-oxalate is characteristic of Zr itself with a strong affinity for the bones and the joints (see PET image, Fig. 5).

In the case of [^{89}Zr]Zr-citrate, the electrophoresis and the biodistribution show some proof of Zr decomplexation. The electrophoretic analysis indicate a significant peak of activity matching with [^{89}Zr]Zr-chloride, and the bone uptake was relatively consequent 6 days p.i. (~13% ID/g).

Zr^{4+} forms an insoluble salt with the phosphate and precipitates in water [2, 19, 21] as observed in Fig. 1.C in which all the activity is concentrated at the origin point of the electrophoreses. The insolubility of [^{89}Zr]Zr-phosphate in water consequently implies a high uptake in the liver and the spleen, persisting after 6 days. The high affinity of Zr^{4+} to phosphonate is also in line with the bone uptake results observed for [^{89}Zr]Zr-chloride. In fact, this affinity seems to be so strong that only a couple of percent of the bone activity is released and cleared from the body after 6 days.

The concentration of [^{89}Zr]Zr-oxalate injected in this study is 10 mM (V=200μL) close to the mice LD50 of oxalate: 155 mg/kg (1.8 mmol/kg) via intraperitoneal injection [22]. In addition, oxalate is reported as a potential neuro and cardiotoxic agent in humans [23] [24]. Therefore, looking upon the similar biodistribution of [^{89}Zr]Zr-chloride and [^{89}Zr]Zr-oxalate and knowing the strong toxicity of this latest, [^{89}Zr]Zr-chloride would preferably be used to [^{89}Zr]Zr-oxalate for a potential medical purpose.

The decreasing blood activity, the constant bone activity and the absence of activity in the marrow compartment are strong evidences that free ^{89}Zr is specifically accumulated in the non-soft tissue, mineralized constituents of the bone. The information provided by the bone dissection and the PET imaging (Fig. 5-[^{89}Zr]Zr-chloride and [^{89}Zr]Zr-oxalate) shows that the epiphysis, mostly constituted of cartilage, carry the majority of the bone activity. This result is in line with a statement of Wuthier, R.E et al [25], explaining the high mineral content in the matrix of calcified cartilage compare to bone in calf. It is very likely that ^{89}Zr is chelated by hydroxylapatite, phosphates constituents of bones and epiphysis [26]. This

hypothesis is also confirmed by the strong affinity of ^{89}Zr with the phosphate observed when Zr was dissolved in PBS.

In the present study, [^{89}Zr]Zr-DFO was immediately cleared from the system, without any sign of bone uptake. In the context of [^{89}Zr]Zr-DFO-traztuzumab administration, the hypothesis that specific cleavage of the intact [^{89}Zr]Zr-DFO from the antibody would not lead to Zr bone uptake as it would immediately be excreted. Indeed, previous studies investigating [^{89}Zr]Zr-DFO-traztuzumab biodistribution in mice show an increasing accumulation of activity in the bones starting at 24h p.i.. This reaches a peak of approximately 10% ID/g after 6 days p.i. [9, 27, 28], in line with the bone uptake of [^{89}Zr]Zr-chloride presently observed of 16% ID/g at the same time reference. The Zr bone uptake is not particularly noticeable in humans [29] and so it is unlikely that Zr is released from the DFO-traztuzumab conjugate while in circulation. More probable is the faster metabolism of the mouse together with its less specific peptidases involving rapid degradation of [^{89}Zr]Zr-DFO and the release of Zr into the circulation. This question remains to be resolved and it is an ongoing study with clinical investigations in patients regarding the metabolism of the labeled ^{89}Zr-mAb and comparing these results with those of the mouse model used herein.

CONCLUSION

Despite the complexity of Zr coordination, the electrophoretic analyses provided detailed evidences of different zirconium preparations charges, salts or complexes.

This study also shows that weakly chelated ^{89}Zr is a bone seeker. The observed rank order of bone uptake was chloride>oxalate>citrate≫DFO which is consistent with the denticity of the chelates and the stability of the respective complexes. The intravenous (i.v.) administration of [^{89}Zr]Zr-phosphate resulted in little bone uptake because of the trapping of the precipitate in the liver and spleen and its negligible bioavailability. It is possible that the observed high murine bone uptake of ^{89}Zr following i.v. administration of ^{89}Zr labeled mAbs is due to the metabolism of the [^{89}Zr]Zr-DFO by the less selective enzymes of the mouse liver.

Even if [^{89}Zr]Zr-oxalate and [^{89}Zr]Zr-chloride revealed very similar biodistribution profiles, especially after 24h p.i., [^{89}Zr]Zr-chloride should be preferred for a potential medical application to its oxalate complex because of the high toxicity of oxalate reported for human and animals [24].

Finally, the strong affinity of zirconium to phosphates may be informative for new opportunities in ligands design complexing this radionuclide in a higher kinetic stability than DFO.

Acknowledgments

We would like to thanks the following institutions: Geoffrey Beene Cancer Research Center of Memorial Sloan-Kettering Cancer Center (JSL); the Office of Science (BER), U. S. the Department of Energy (Award DE-SC0002456; JSL), Mr. William H. Goodwin and Mrs. Alice Goodwin and the Commonwealth Foundation for Cancer Research, the Experimental Therapeutics Center of Memorial Sloan-Kettering Cancer Center; and the

technical services provided by the MSKCC Small-Animal Imaging Core Facility supported in part by NIH grants R24 CA83084 and P30 CA08748. The authors would also like to sincerely acknowledge the kind participation of Prof. J. Lewis, Dr. J. Holland. Many thanks are also addressed to Dr E. Santos, Dr D. Ulmert and Dr D. Thorek for their scientific discussions and corrections.

References

1. Chisholm, H. Zirconium. In: Britannica, TE., editor. The Encyclopaedia Britannica: a dictionary of arts, sciences, literature and general information. 11. New York: The Encyclopaedia Britannica Compagny; 1911. p. 990
2. Steinberg EP. The Radiochemistry of Zirconium and Hafnium. National Academy of Sciences - National Research Councyl - Nuclear Sciences Series. 1960
3. Review of Specific Radionuclides - Zirconium. Multi-Agency Radiological Laboratory Analytical Protocols Manual (MARLAP). 2004:369–76.
4. Sasaki T, Kobayashi T, Takagi I, Moriyama H. Hydrolysis Constant and Coordination Geometry of Zirconium(IV). Journal of Nuclear Science and Technology. 2008; 45(8):735–9.
5. McClinton L, Schubert J. The Toxicity of some Zirconium and Thorium salts in Rats. J Pharmacol Exp Ther. 1948; 94(1):1–6. [PubMed: 18885606]
6. Sastry BV, Owens LK, Ball CO. Differences in the Distribution of Zirconium-95 and Niobium-95 in the Rat. Nature. 1964 Jan 25.201:410–1. [PubMed: 14110018]
7. Backstrom J, Hammarstrom L, Nelson A. Distribution of Zirconium and Niobium in Mice. Acta Radiologica Therapy Physics Biology. 1967; 6(2):122–8.
8. Meijs WE, Haisma HJ, Klok RP, vanGog FB, Kievit E, Pinedo HM, et al. Zirconium-labeled monoclonal antibodies and their distribution in tumor-bearing nude mice. Journal of Nuclear Medicine. 1997 Jan; 38(1):112–8. [PubMed: 8998164]
9. Holland JP, Divilov V, Bander NH, Smith-Jones PM, Larson SM, Lewis JS. 89Zr-DFO-J591 for immunoPET of prostate-specific membrane antigen expression in vivo. J Nucl Med. 2010 Aug; 51(8):1293–300. [PubMed: 20660376]
10. Holland JP, Caldas-Lopes E, Divilov V, Longo VA, Taldone T, Zatorska D, et al. Measuring the pharmacodynamic effects of a novel Hsp90 inhibitor on HER2/neu expression in mice using Zr-DFO-trastuzumab. PLoS One. 2010; 5(1):e8859. [PubMed: 20111600]
11. Ruggiero A, Holland JP, Lewis JS, Grimm J. Cerenkov luminescence imaging of medical isotopes. J Nucl Med. 2010 Jul; 51(7):1123–30. [PubMed: 20554722]
12. Perk LRVM, Visser GW, Budde M, Jurek P, Kiefer GE, van Dongen GA. p-Isothiocyanatobenzyl-desferrioxamine: a new bifunctional chelate for facile radiolabeling of monoclonal antibodies with zirconium-89 for immuno-PET imaging. Eur J Nucl Med Mol Imaging. 2010; 37(2):250–9. [PubMed: 19763566]
13. Smith-Jones PM. Unpublished data.
14. Smith-Jones PM, Vallabhajosula S, Navarro V, Bastidas D, Goldsmith SJ, Bander NH. Radiolabeled monoclonal antibodies specific to the extracellular domain of prostate-specific membrane antigen: preclinical studies in nude mice bearing LNCaP human prostate tumor. J Nucl Med. 2003 Apr; 44(4):610–7. [PubMed: 12679407]
15. Holland JP, Sheh YC, Lewis JS. Standardized methods for the production of high specific-activity zirconium-89. Nucl Med Biol. 2009 Oct; 36(7):729–39. [PubMed: 19720285]
16. Research IfLA. Guide for the Care and Use of Laboratory Animals. Washington, D.C: The National Academy Press; 1996.
17. Mealey J. Turn-over of Carrier-Free Zirconium-89 in Man. Nature. 1957; 179(4561):673–4. [PubMed: 13418761]
18. Mazzi, UEWC.; Volkert, WA., editors. Technetium and Other Radiometals in Chemistry and Medicine. Padova: Servizi Grafici Editoriali snc; 2010.
19. Ghosh SSA, Talukder G. Zirconium An Abnormal Trace Elelment in Biology. Biological Trace Element Research. 1992; 35:247–71. [PubMed: 1283692]

20. Meijs WE, Haisma HJ, VanderSchors R, Wijbrandts R, VandenOever K, Klok RP, et al. A facile method for the labeling of proteins with zirconium isotopes. Nucl Med Biol. 1996 May; 23(4): 439–48. [PubMed: 8832698]

21. Osanai T, Hayakawa K, Kikushi N, Konno S, Ito K, Shibata N, et al. Investigation of Interference by Inorganic Phosphate on Coprecipitation of Cadmium, Copper, Manganese and Lead in Water with Zirconium Hydroxide Pharmaceutical Society of Japan. 1989; 35(4):297–300.

22. Klinger W, Kersten L. Studies on the effect of calcium thiosulfate and dicalcium- and disodium versenate. II. Protective action against lead and oxalate poisoning and alteration of membrane permeability. Acta biologica et medica Germanica. 1961; 6:498–508. [PubMed: 14457026]

23. L'Epée P, Castagnou R, Larcebau S, Lazarini H, Doignon J. Intoxication aiguë mortelle par l'oxalate neutre de potassium. Médecine légale et dommage corporel. 1971; 4:178–81. [PubMed: 5315066]

24. Gamelin LCO, Morel A, Dumont A, Traore S, Anne le B, Gilles S, Boisdron-Celle M, Gamelin E. Predictive factors of oxaliplatin neurotoxicity: the involvement of the oxalate outcome pathway. Clin Cancer Res. 2007 Nov 1; 13(21):6359–68. [PubMed: 17975148]

25. Wuthier RE. A Zonal Analysis of Inorganic and Organic Constituents of the Epiphysis during Endochondral Calcification. Calcified Tissue International. 1969; 4(1):20–38.

26. Khurana, JS., editor. Bone Pathology. 2. New York: Human Press; 2009.

27. Tinianow JN, Gill HS, Ogasawara A, Flores JE, Vanderbilt AN, Luis E, et al. Site-specifically Zr-89-labeled monoclonal antibodies for ImmunoPET. Nucl Med Biol. 2010 Apr; 37(3):289–97. [PubMed: 20346868]

28. Dijkers ECF, Kosterink JGW, Rademaker AP, Perk LR, van Dongen GAMS, Bart J, et al. Development and Characterization of Clinical-Grade Zr-89-Trastuzumab for HER2/neu ImmunoPET Imaging. Journal of Nuclear Medicine. 2009 Jun 1; 50(6):974–81. [PubMed: 19443585]

29. Dijkers EC, Oude Munnink TH, Kosterink JG, Brouwers AH, Jager PL, de Jong JR, et al. Biodistribution of 89Zr-trastuzumab and PET imaging of HER2-positive lesions in patients with metastatic breast cancer. Clin Pharmacol Ther. 2010 May; 87(5):586–92. [PubMed: 20357763]

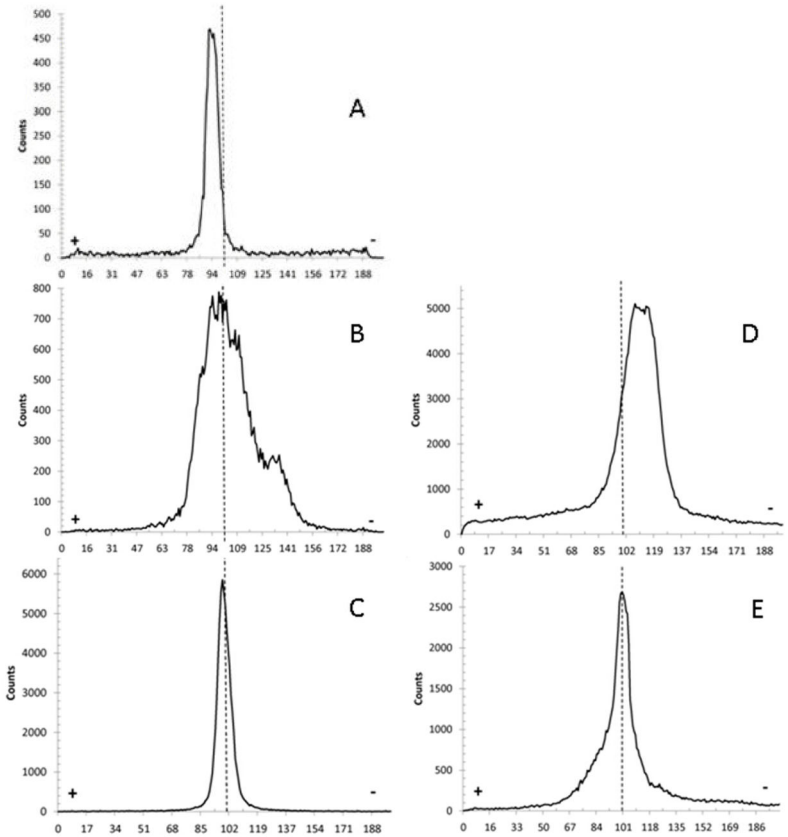

Fig. 1.

Electrophoresis chromatograms for [^{89}Zr]Zr-chloride (A); [^{89}Zr]Zr-oxalate (B); [^{89}Zr]Zr-phosphate (C); [^{89}Zr]Zr-DFO (D); [^{89}Zr]Zr-citrate (E). Each dashed line indicated where the original ^{89}Zr was spotted prior to electrophoresis.

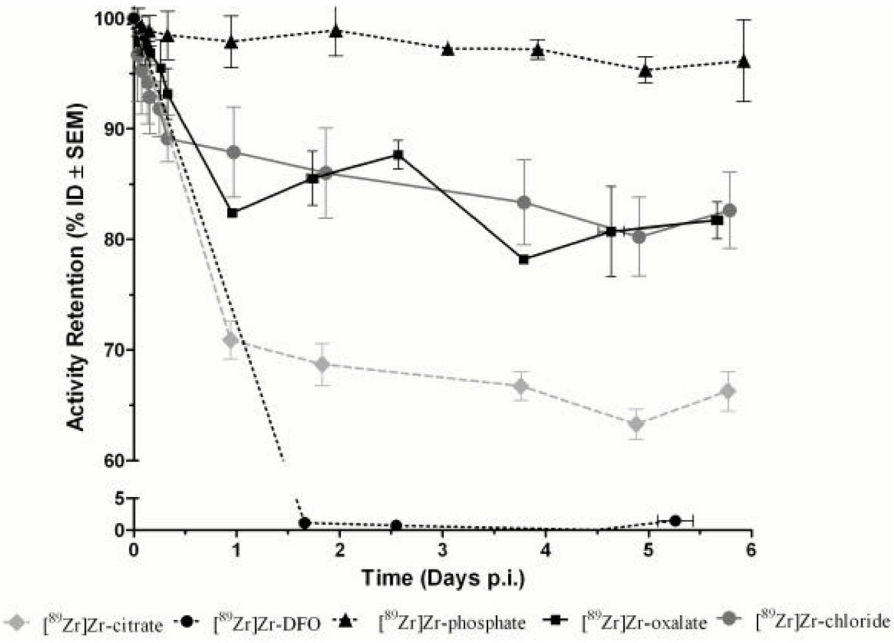

Fig. 2.

Whole body retention of radioactivity in female NIH Swiss mice (n≥3) following i.v. administration of various chemical forms of ^{89}Zr (note the axis break).

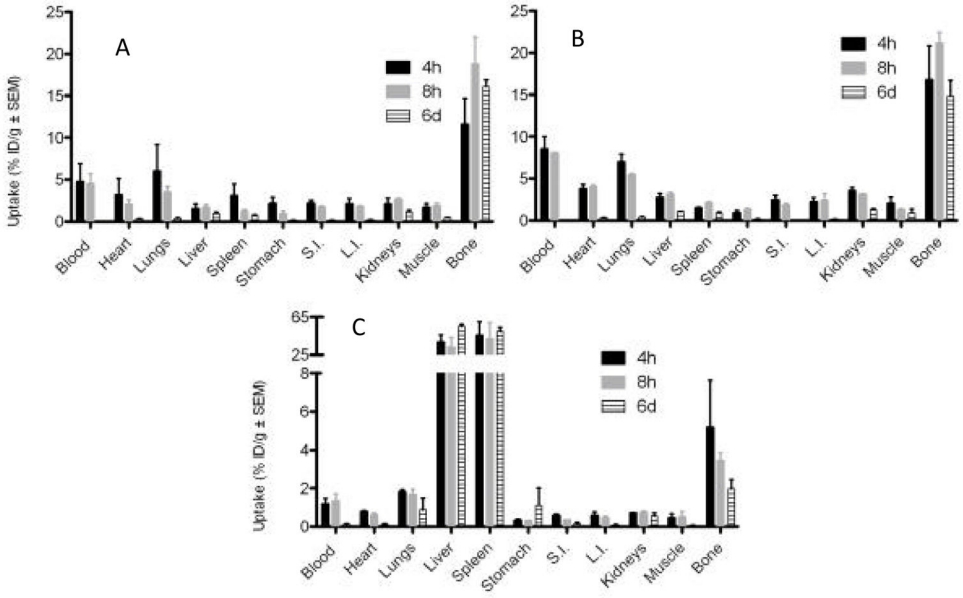

Fig. 3.

Biodistribution of radioactivity following i.v. administration of various chemical form of ^{89}Zr (740 KBq in 200 μL) in female NIH swiss mice (n≥3). A-[^{89}Zr]Zr-chloride; B-[^{89}Zr]Zr-oxalate; C[^{89}Zr]Zr-phosphate (note the axis break; S.I.: Small Intestine; L.I.: Large Intestine).

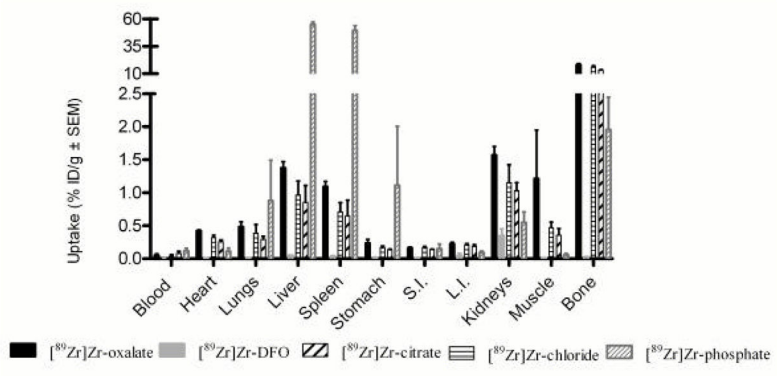

Fig. 4.

Biodistribution of radioactivity at 6 days p.i. following i.v. administration of various chemical form of ^{89}Zr (740 KBq in 200 μL) in female NIH swiss mice (n≥3; note the axis break).

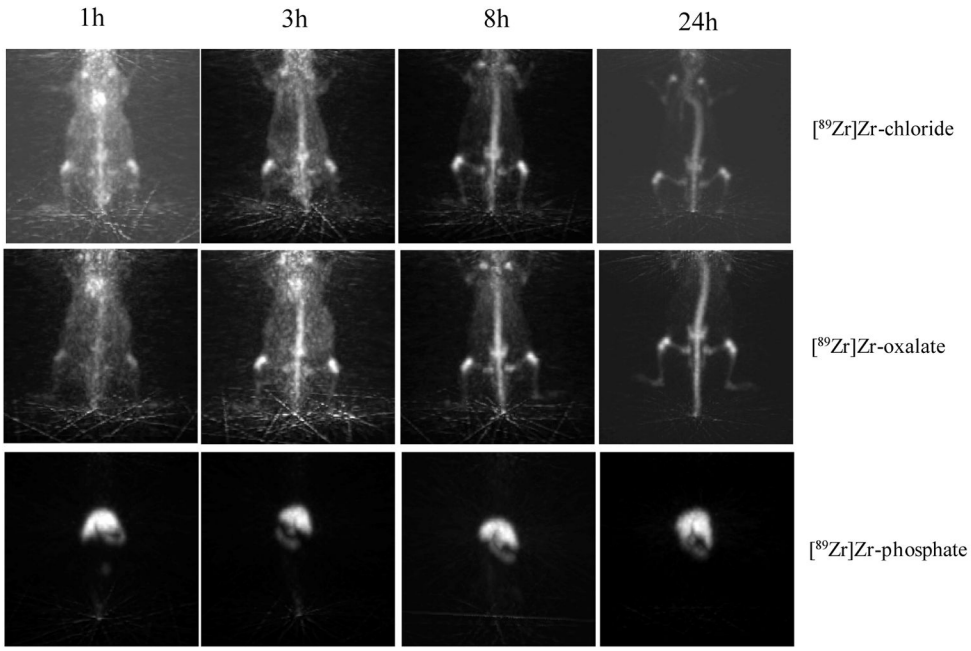

Fig. 5.

Serial projection PET images acquired with 10 min scan length at 1, 3, 8 and 24 h p.i. of [^{89}Zr]Zr-chloride; [^{89}Zr]Zr-oxalate or [^{89}Zr]Zr-phosphate (740 KBq in 200 μL) in normal female NIH Swiss mice (anesthesized with 1% isoflurane/oxygen 2 L.min^{-1}).